Depth domain inversion to improve the fidelity of subsalt imaging: a Gulf of Mexico case study

Laurence Letki[1*], Jun Tang[1], Charles Inyang[1], Xiang Du[1] and Robin Fletcher[1] describe a depth domain inversion workflow that produces an acoustic impedance volume corrected for illumination effects, thus providing more consistent and reliable rock property attributes from depth-migrated datasets.

Accurate geophysical reservoir characterisation in complex geologic environments remains a challenge. In particular, conventional methods of amplitude inversion assume that amplitudes in the seismic image are correctly located and can be inverted to elastic parameters from which a true representation of rock properties can be derived. However, complex geology, often combined with limitations imposed by surface seismic acquisition geometries, can lead to inadequate illumination of subsurface targets, which can have detrimental effects on the amplitudes and phase of the migrated image.

Conventional amplitude inversion techniques do not compensate for these amplitude and phase variations. Consequently, imprints of various non-geological effects and a complex overburden will manifest themselves in the results of seismic inversion, leading to less reliable estimation of acoustic and elastic parameters.

An additional challenge to accurate amplitude inversion in complex geologic environments is that depth imaging is normally required to obtain a reliable image of the subsurface, while current amplitude inversion techniques are usually implemented in the time domain. This difference in approach between the imaging and inversion steps can compromise the fidelity of the attributes derived from seismic inversion.

In order to improve consistency between structural imaging and rock property estimation, a technique has been developed to perform amplitude inversion directly in the depth domain. The inversion workflow uses point spread functions to capture and correct for space-, depth- and dip-dependent illumination effects resulting from the acquisition geometry and complex geology. The amplitude inversion is performed in the depth domain and the output is a reflectivity image and associated acoustic impedance volume corrected for illumination effects, thus creating more consistent and reliable imaging products and rock property attributes from depth-migrated datasets. This article presents the application of the depth domain inversion workflow to a long-offset full-azimuth (FAZ) dataset from the Green Canyon area of the Gulf of Mexico (GoM) (Letki et al., 2015).

Long-offset full-azimuth data

Several areas of the GoM present severe imaging challenges related to thick salt sheets with complex morphology. Modelling studies have indicated that to adequately image subsalt in these areas requires not only FAZ coverage but also long source-receiver offsets. The Dual Coil Shooting multi-vessel full-azimuth acquisition design has been developed to achieve these requirements. It involves two recording vessels with their own sources and two separate source vessels sailing in large interlinked circles (Figure 1). In addition to full 360 degree subsurface illumination, the configuration delivers a trace density approximately 2.5 times that of current wide-azimuth survey designs, which improves signal-to-noise-ratio to further enhance the imaging of weak subsalt reflections.

Schlumberger has acquired and processed more than 30,000 km^2 of long-offset (up to 14 km) FAZ data – equivalent to almost 1300 Outer Continental Shelf (OCS) blocks – in its Revolution programme of multi-client surveys in the deepwater GoM. The processing sequence included true-azimuth 3D general surface multiple prediction (3D GSMP) and velocity model building incorporating tilted transverse anisotropy (TTI). Standard deliverables include anisotropic Kirchhoff and reverse time migration (RTM) volumes.

Full waveform inversion (FWI) has proven to be a valuable tool for improving the accuracy of subsurface velocity models for the Revolution surveys, where imaging challenges include the need to address anisotropy. The long offsets provided by the Dual Coil Shooting acquisition method are of particular benefit in helping FWI to enhance the velocity model in the suprasalt section and within the mini-basins. Furthermore, longer offsets mitigate the sensitivity of the inversion process to the initial velocity model by enabling FWI to update the low wavenumber component.

Illumination challenges

This case study used data from part of the K2 area of the Revolution II multi-client survey. Full azimuthal and long offset coverage has optimised the imaging of the target and

[1] *Schlumberger.*

[*] *Corresponding author, E-mail: LLetki@slb.com*

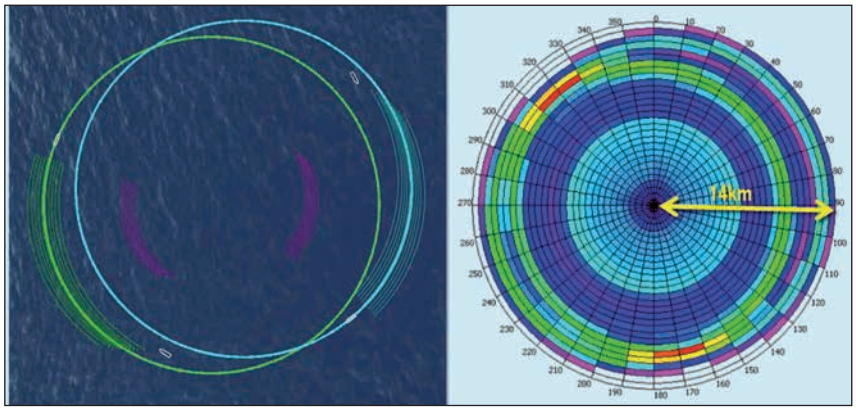

Figure 1 *The Dual Coil Shooting acquisition design used for the Revolution programme involves two recording vessels with their own sources and two separate source vessels sailing in large interlinked circles. The configuration delivers full 360 degree subsurface illumination, long offsets, and a trace density approximately 2.5 times that of current wide-azimuth survey designs.*

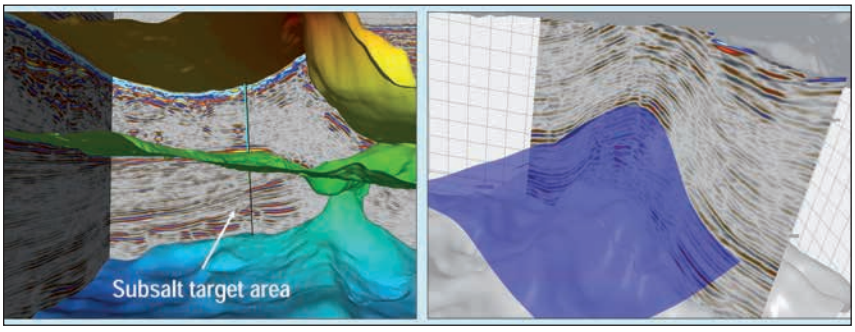

Figure 2 *Illustration of the subsalt target area (left) and an RTM image with source illumination compensation through the target area overlaid in blue with the interpretation of the target horizon (right).*

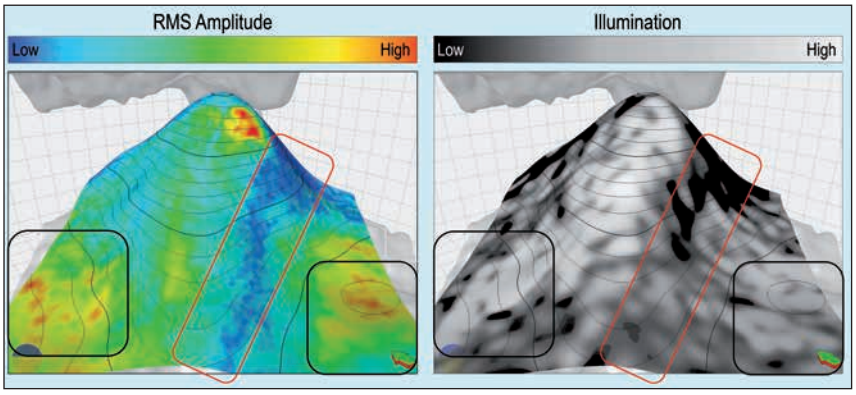

Figure 3 *RMS amplitude extracted around the target horizon (left) and illumination map at target horizon (right). The area outlined in red is a corridor of low illumination that corresponds to a low amplitude corridor in the RTM image. The areas outlined in black have high amplitudes in the RTM image that correspond to areas of high illumination.*

interpretation of key subsalt horizons in the RTM data volume (Figure 2). However, the target in this area is poorly illuminated due to the complexity of the salt overburden. This inadequate subsurface illumination has detrimental effects on the amplitudes and phase of the migrated image.

Analysis of the amplitudes extracted along key horizons shows a correlation with variations in illumination (Figure 3). Areas that are well illuminated with a wide range of offsets and azimuths tend to correspond to higher amplitudes. By contrast areas illuminated by a more restricted range of offsets and azimuths tend to correspond to low amplitude areas along the key horizon. Conventional amplitude inversion techniques do not compensate for these variations in amplitude, and also phase. The imprint of non-geological effects, including illumination, in the results of seismic inversion imposes a significant limitation for quantitative interpretation. Consequently, any attributes derived from amplitudes in the seismic image volume will not accurately represent the properties of the corresponding lithology.

Capturing dip-dependent illumination effects using point spread functions

A new technique was applied to the test dataset that performed amplitude inversion directly in the depth domain. The method was designed to correct for spatial, depth and dip-dependent illumination effects related to both acquisition geometry and complex geology. The objective was to create more reliable seismic inversion attributes that were also more consistent with the depth imaging products.

The key input to the workflow was a grid of point spread functions (PSFs). These are the impulse response of the modelling and imaging procedure. The migrated image $\boldsymbol{m}$ is related to the true reflectivity $\boldsymbol{r}$ by $\boldsymbol{m = M^*Mr = Hr}$ where $\boldsymbol{M}$ is a modelling operator, $\boldsymbol{M^*}$ is the migration operator and $\boldsymbol{H=M^*M}$ is a Hessian operator, a measure of the illumination effects due to velocity variations and acquisition geometry, which blurs the true reflectivity to give the migrated image. The grid of PSFs is an approximation of the Hessian operator. In other words, it is a representation of the spatially and depth variant 3D wavelet embedded in the migrated image and it captures the dip-dependent illumination effects due to acquisition geometry and complex geology.

Careful analysis of the information captured by the PSFs can be correlated with the amplitude and phase variations observed along the target horizon. Figure 4 presents example inline and crossline displays through the RTM volume. The PSF corresponding to an area with lower amplitudes has been extracted and analysed. The K_xK_z and K_yK_z spectra of this PSF clearly illustrate strong dip dependence. The geological dip estimated from the RTM image, shown overlaid on the spectra of the corresponding PSF, lies at the edge of the illuminated dip range. This example observation confirms the effects of variable illumination on the RTM image.

Depth domain inversion workflow

The depth domain inversion workflow finds the best acoustic impedance and associated reflectivity model $\boldsymbol{r}$ by minimising the least squares objective function $\|\boldsymbol{m - Hr}\|^2$ (Fletcher et al., 2012). It is entirely performed in the depth domain. Prior to running the inversion, the PSFs are calibrated at well locations using an extracted residual wavelet. This residual wavelet accounts for effects not modelled during the PSF generation and ensures an optimum match between the seismic data and the well data. As wavelet variations caused by illumination effects have been modelled by the PSFs, the

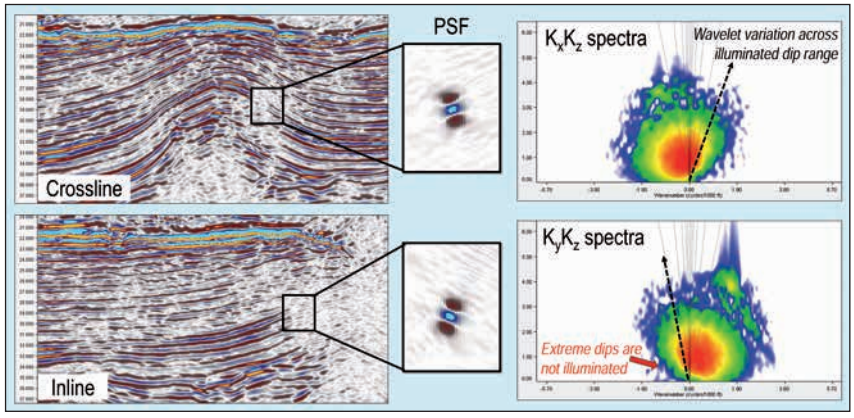

Figure 4 *Inline and crossline through the RTM image (left). Inline and crossline through the corresponding PSF extracted at the highlighted location (middle). Associated Kx Kz and Ky Kz spectra (right) showing the dip-dependent illumination effects captured by the PSF. The estimated local geological dip is represented by the black arrow.*

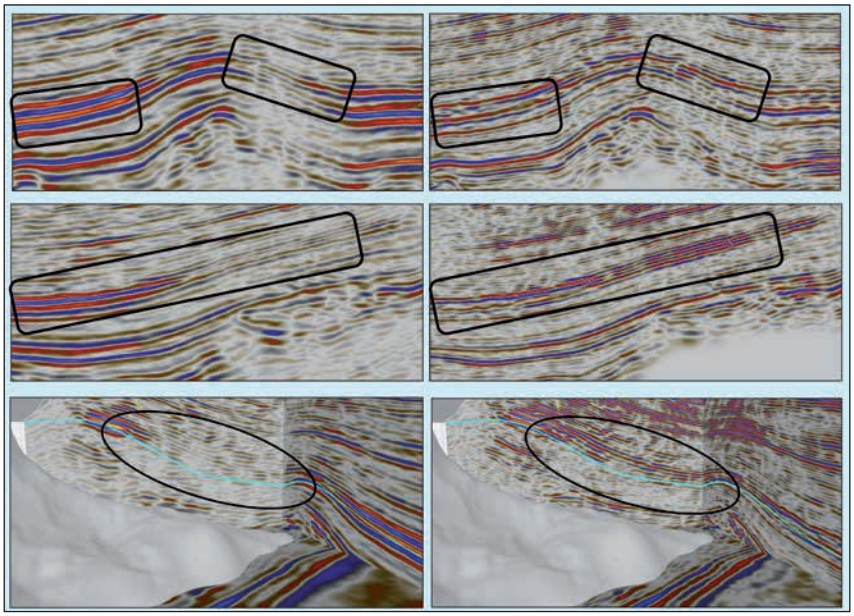

Figure 5 *Example RTM images with source illumination compensation (left) compared to equivalent reflectivity images output from the depth domain inversion (right). The black rectangles in the top and middle sections outline some high- and low-amplitude areas in the RTM image that have more balanced amplitudes in the reflectivity image. The area in the bottom panels outlined in a black oval is an example of where structural interpretation can be significantly improved after depth domain inversion.*

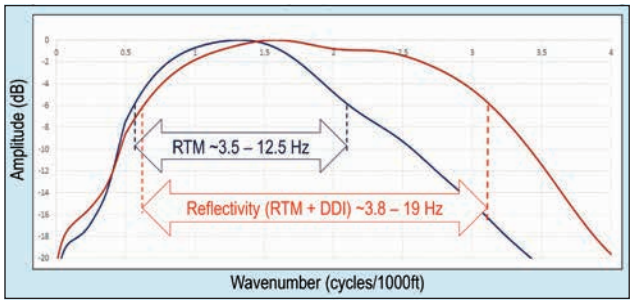

Figure 6 *Amplitude spectra extracted along the target horizon from the RTM image (blue) and the reflectivity image (red), normalised to maximum amplitude. The reference frequency ranges are calculated from the wavenumbers and the approximate velocity within the analysis window.*

underlying assumption that the residual wavelet is stable in time is much more appropriate than for conventional time domain inversion.

The output from depth domain inversion is a reflectivity image corrected for the dip-dependent illumination effects and, when appropriate well data is available for calibration, the associated absolute acoustic impedance volume. Additional constraints that can be included in the objective function relate to sparsity of the reflectivity model, lateral continuity of the output along the geological structure, and deviation from a prior low-frequency model.

Depth domain inversion results

Figure 5 compares example RTM images with source illumination compensation with the reflectivity images resulting from depth domain inversion. The inversion has provided clear improvement in the continuity of major events, delivered overall sharpening of the image, and revealed details of minor events previously unseen. As shown in Figure 6, there is also a significant increase in bandwidth, as the wavelet embedded in the RTM image is deconvolved to lead to the reflectivity image. The spectra of the reflectivity image does not extend further because the dataset used in this example was only migrated up to 25Hz.

Figure 7 compares RMS amplitudes extracted along the key horizon from the RTM image before and after correction for dip-dependent illumination effects (the reflectivity image). The amplitudes in the reflectivity image appear more balanced, less impacted by the variable illumination, and more consistent with the subsurface structure. It should be noted that in areas of very low illumination, the amplitudes on the reflectivity image remain low as the signal-to-noise-ratio is insufficient for adequate illumination compensation. Another limitation of the inversion results appears around high acoustic impedance contrasts, such as the salt boundaries in this case study. The PSF discontinuity across such a high contrast boundary is very high and a simple interpolation of the PSFs is not appropriate. In this situation a more sophisticated interpolation scheme, a denser PSF grid, or a combination of both is required.

An increased reliability in the seismic amplitudes leads to an increased reliability in the acoustic impedance results of the depth domain inversion. Figure 8 compares the acoustic impedance volume obtained from the RTM image using a conventional time domain inversion approach, with the results obtained from the depth domain approach. The variable illumination effects directly impact the time domain inversion results, with low amplitudes being wrongly inverted into low reflectivity. The acoustic impedance volume resulting from the depth domain inversion is corrected for these effects, leading to more consistent acoustic impedance layers. These results illustrate how depth domain inversion can improve the fidelity of both structural and quantitative interpretation of complex subsalt targets.

Conclusions

The depth domain inversion workflow illustrated in this article used point spread functions to capture space, depth- and dip-dependent effects related to acquisition geometry and complex geology. The amplitude inversion was performed in the depth domain and the output was a reflectivity image and associated acoustic impedance volume corrected for illumination effects. The resulting reflectivity image provides better event continuity, a sharper image and more reliable amplitude information, associated with a higher fidelity

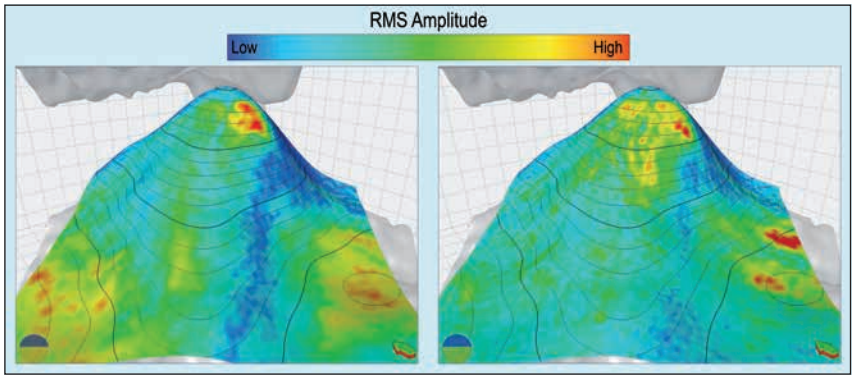

Figure 7 *RMS amplitude extracted around the target horizon on the RTM image (left) showing a strong imprint of the illumination effects. The RMS amplitude extracted around the target horizon on the reflectivity image (right) shows better consistency of the amplitudes with the structure of the horizon and a significantly reduced imprint of the variable illumination.*

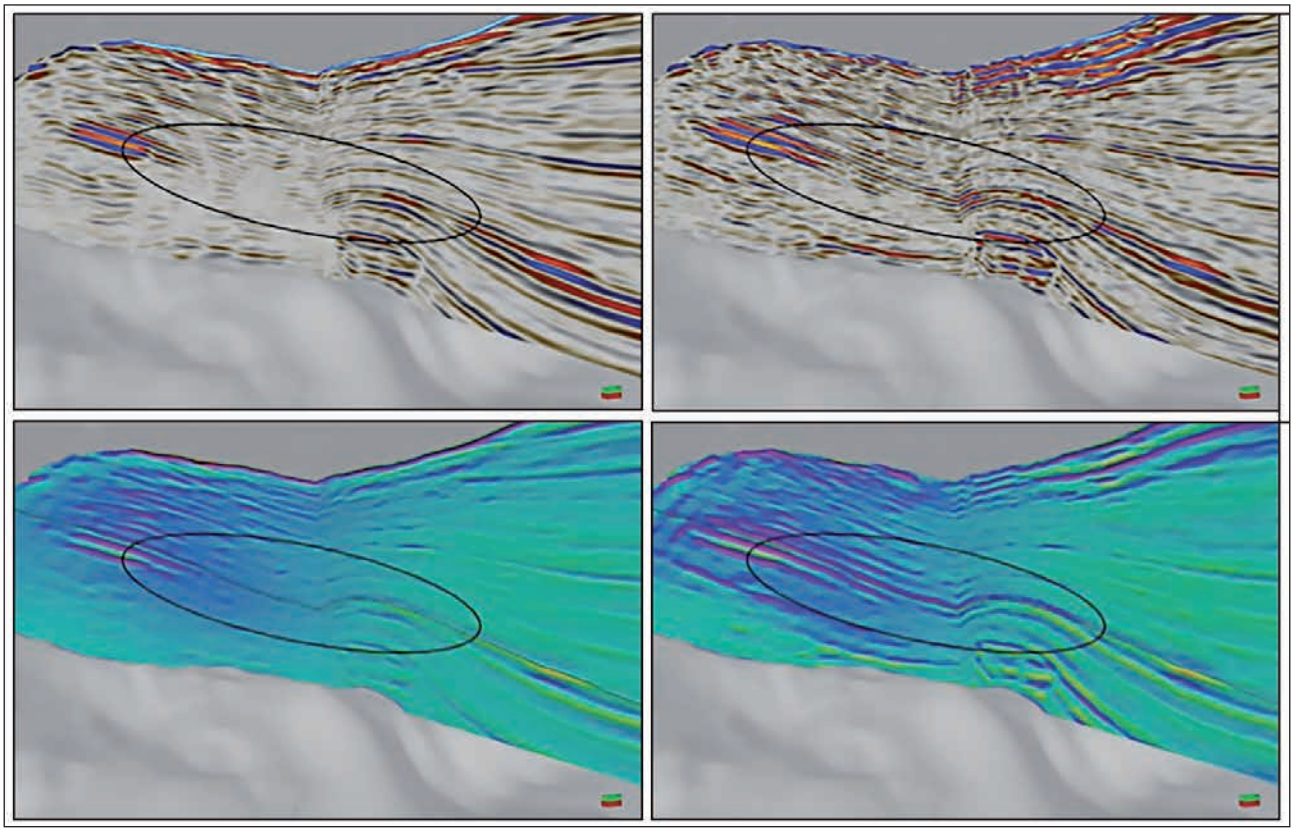

Figure 8 *The upper panels show an example RTM image with source illumination compensation (left) compared to reflectivity image output from the depth domain inversion (right). The lower panels show acoustic impedance volumes from the time domain inversion (left) and depth domain inversion (right), annotated with an interpretation of a key horizon. A comparison of the areas highlighted in the black ovals in the top panels demonstrates how structural interpretation can be significantly improved after depth domain inversion. The same area is highlighted in the bottom panels to highlight how quantitative interpretation is also improved after depth domain inversion (Includes data supplied by IHS Energy Log Services, Inc.; copyright (2015) IHS Energy Log Services, Inc.).*

acoustic impedance volume. This enables an improved structural and quantitative interpretation. There is also the option to include more sophisticated physics in the generation of the PSFs, to incorporate ghost effects (Caprioli et al., 2014) or attenuation effects (Cavalca et al., 2015). Including such aspects within the inversion provides a mechanism to produce an even higher fidelity reflectivity and acoustic impedance image.

Acknowledgements

The authors would like to thank Schlumberger for giving permission to publish this work. All images are courtesy of Schlumberger Multiclient.

References

Cavalca, M., Fletcher, R.P. and Du, X. [2015] Q-compensation through depth domain inversion. *77th EAGE Conference & Exhibition*, Extended Abstracts.

Caprioli, P.B.A., Du, X., Fletcher, R.P. and Vasconcelos, I. [2014] 3D source deghosting after imaging. *84th Annual International Meeting, SEG*, Expanded Abstracts, 4,092-4,096.

Fletcher, R.P., Archer, S., Nichols, D. and Mao, W. [2012] Inversion after depth imaging. *82nd Annual International Meeting, SEG*, Expanded Abstracts, 1-5.

Letki, L.P., Tang, J. and Du, X. [2015] Depth Domain Inversion Case Study in Complex Subsalt Area. *77th EAGE Conference & Exhibition*, Extended Abstracts.